Lab on a Chip

Accepted Manuscript

ROYAL SOCIETY OF CHEMISTRY

www.rsc.org/loc

ARTICLE TYPE www. rsc.org/xxxxxx | XXXXXXXX

Capacitive deionization on-chip as a method for microfluidic sample preparation

Susan H. Roelofs,*[a], Bumjoo Kim[b], Jan Eijkel[a], Jongyoon Han[b], Albert van den Berg,[a] and Mathieu Odijk[a]

Received Xth XXXXXXXXXX 20XX, Accepted Xth XXXXXXXXX 20XX
First published on the web Xth XXXXXXXXXX 200X
DOI: 10.1039/b000000x

Desalination as a sample preparation step is essential for noise reduction and reproducibility of mass spectrometry measurements. A specific example is the analysis of proteins for medical research and clinical applications. Salts and buffers that are present in samples need to be removed before analysis to improve the signal-to-noise ratio. Capacitive deionization is an electrostatic desalination (CDI) technique which uses two porous electrodes facing each other to remove ions from a solution. Upon the application of a potential of 0.5 V ions migrate to the electrodes and are stored in the electrical double layer. In this article we demonstrate CDI on a chip, and desalinate a solution by the removal of 23% of Na^+ and Cl^- ions, while the concentration of a larger molecule (FITC-dextran) remains unchanged. For the first time impedance spectroscopy is introduced to monitor the salt concentration in situ in real-time in between the two desalination electrodes.

1 Introduction

Sample preparation on-chip is essential to increase throughput, reproducibility[1] and improve the detection limit of lab-on-chip analysis methods. A benefit of lab-on-chip technology is the ability to analyze small sample volumes in the nano- and picoliter range. To optimally exploit this benefit, the required pretreatment steps of the samples must be compatible with these small volumes as well[1,2].

A specific example of an analyzing method for which sample pretreatment is important, is the analysis of biological samples through mass spectrometry (MS) as e.g. in the application of protein analysis for medical research or clinical applications[3,4]. For online monitoring electrospray ionization is a favored method which can be utilized in conjunction with the mass spectrometer. For samples with a high concentration of buffers and salts analysis of spectra is impossible due to a low signal-to-noise ratio also known as ion suppression[5–9]. Additionally, variations in sequential measurements are introduced through manual handling of the sample during pretreatment[1,10], which causes sample loss and contamination[11]. The most commonly applied methods for desalting protein samples are protein extraction through e.g. filters, liquid-chromatography (LC)[12] and solid-phase extraction (SPE)[9], which typically operate with volumes in the microliter range. Previous experiments of desalination on-chip, as a sample preparation method, utilized membranes to extract proteins from the buffer solution[4,7,13–15]. Our approach is to avoid membranes and to apply a robust electrode geometry to extract salts from the solution.

Capacitive deionization (CDI) is an electrostatic desalination technique, which employs two porous electrodes facing each other, with the salt solution flowing in between them[16,17]. Upon the application of a potential of approximately 1.2 V between the electrodes, ions with a high electrophoretic mobility in the solution migrate to the electrodes and are stored in the electrical double layer[18]. Larger molecules with a lower mobility, such as proteins, will take more time to migrate to the electrodes[8,19]. The difference in mobility between the salt ions and the proteins can be utilized to separate them. The mobility of proteins is amongst others dependent on pH and the solution ionic strength[19], which can be tuned to optimize the separation efficiency. Koster et al. concluded in their review that electrospray ionization MS requires flow rates in the order of several nL min^{-1} to μL min^{-1}, which matches well with typical flow rates in microfluidics[20]. Issues with possible electrical interference of the ESI tip voltage can be prevented using a MS with the ESI tip at ground potential, while the MS orifice is operated at high voltage[21].

CDI is already commercially available for macro-scale systems. CDI is potentially energetically favorable for desalination of brackish water compared to more established methods such as reverse osmosis (RO), multi-stage flash distillation (MSF) or electrodialysis (ED)[18] and has therefore raised interest as a potential solution to the increasing drinking water shortage[22]. Recently CDI has been applied on a chip by using pseudo-porous as well as porous electrodes[23,24]. Suss et al. have visualized the transport of Cl^- ions through fluorescence

† Electronic Supplementary Information (ESI) available: [Calculation CDI model. fluorescence spectroscopy image].See DOI: 10.1039/b000000x/

microscopy, demonstrating that the process is diffusion limited. Time-dependent ion selectivity was analyzed by Zhao et al. who concluded that single valent ions are first absorbed by the electrical double layer and in time replaced with divalent ions[25]. We have studied charging effects and localized pH effects on non-porous electrodes in a lab-on-chip (LOC) in an earlier paper[26].

As a sample preparation method CDI offers several advantages over previously mentioned alternative desalination methods. The regeneration process of CDI is such that it does not require additional solvents as in e.g. ED[27,28]. Additionally, CDI does not suffer from biofouling of membranes as is commonly encountered in membrane techniques such as ED and RO[29]. Also, the flow rate used in CDI is scalable and does not require a high/large pressure pump (RO) nor does CDI require elevated temperatures as in MSF[29]. Due to the clear-cut geometry consisting of few parts, CDI can be readily integrated on-chip.

In this article we demonstrate the application of CDI on-chip as a microfluidic sample preparation method, through desalination of a sample where FITC-dextran is used as model compound for further analysis by MS. Additionally, a novel method is introduced to monitor the salt concentration between the desalination electrodes in a real time manner, based on impedance spectroscopy. This method is combined with fluorescent imaging to demonstrate the desalination of the model compound.

2 Theory

2.1 Cell constant

The cell constant (K) for a typical CDI setup consisting of two electrodes facing each other is given by $K = d/a$, where d [m] is the width of the channel and a [m^2] is the area of the electrodes. The impedance is calculated from $|Z| = \rho \cdot K$, where $|Z|$ [Ω] represents the impedance and ρ[Ω·m] the resistivity.

2.2 Theoretical model of CDI on chip

The salt concentration as a function of time is monitored through impedance measurements at a single frequency using the same set of electrodes that is used to desalinate. These electrodes are 12 mm long and form the side walls of the flow channel, see figure 1. The measurements give an average number of the concentration of NaCl between the electrodes. However, locally the concentration drop and thus the actual desalination percentage is expected to be higher. This hypothesis is supported through the following basic element model, which calculates the concentration C[M] as a function of time (t[s]) at the exit of the desalination electrodes as well as the average concentration measured between the electrodes. A schematic of the model is shown in figure 2. The capacitor, with length L, is divided in n_e elements. Initially each element is filled with the start concentration of 10 mM NaCl. During their residence time between the electrodes the elements are desalinated. Figure 2 shows from left to right the situation at $t = t_1$, t_2 and t_3.

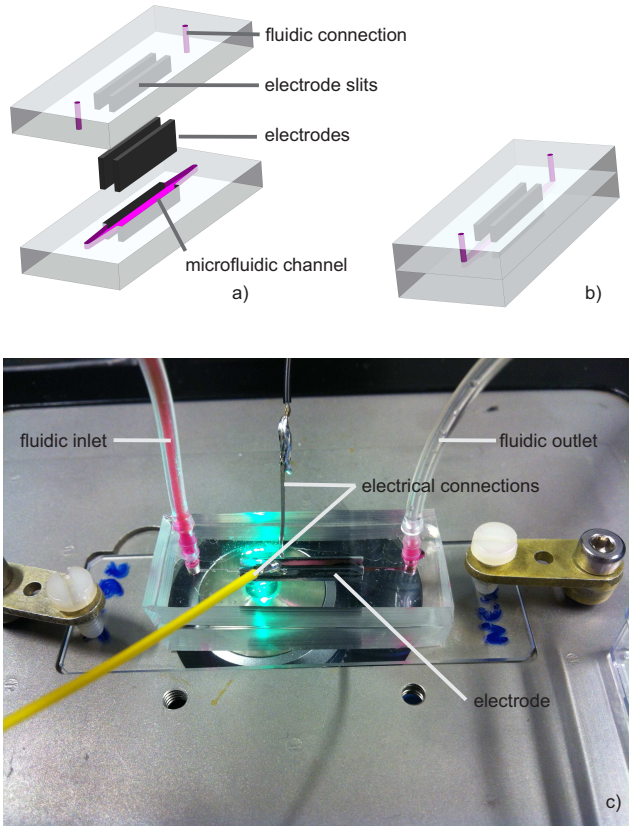

Fig. 1 a) Exploded view of the chip. The fluidic channels are colored in violet. The carbon electrodes are colored black. b) Assembled chip. c) Photograph of the microfluidic chip on a stage from an inverted microscope. The chip is connected to a syringe pump through tygon tubing. Stainless steel wires connect the carbon electrodes to the potentiostat

The salt concentration as a function of time at $x = L$ can be described by:

$$C(t) = C_0 - \frac{\Gamma}{FV}\int_{t_0}^{t_n} I_n dt, \text{for } 0 < t < t_t \qquad (1)$$

and

$$C(t) = C_0 - \frac{\Gamma}{FV}\int_{t_n - t_t}^{t_n} I_n dt, \text{for } t_t < t < t_e, \qquad (2)$$

[a] *BIOS - the Lab-on-a-Chip group, Mesa+ Institute for Nanotechnology, MIRA Institute, University of Twente, P.O. box 217, 7500 AE Enschede, The Netherlands, E-mail: s.h.roelofs@utwente.nl*
[b] *Department of Biological Engineering, Massachusetts Institute of Technology, 77 Massachusetts Avenue, Cambridge, MA, 02139, USA*

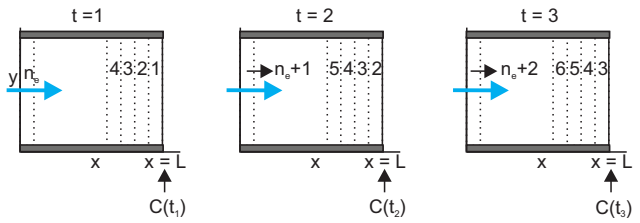

Fig. 2 Schematic of the desalination electrodes for the first three time intervals. The flow direction is indicated with the blue arrow. The concentration C is determined at the exit of the electrodes at $x = L$ for n elements. The number of elements that fit in the capacitor is n_e.

where F is the Faraday constant [C mol^{-1}], V is the volume of a single element [m^3], C_0[mol m^3] is the starting concentration of 10 mM NaCl, t_n[s] is the time, t_t[s] is the residence time of a single element in the capacitor and I_n[A] is the current obtained from the measurements, see the electronic supplementary information (ESI) figure S1, through a single element. The charge efficiency (Γ), which describes the amount of salt absorbed in relation to charge displaced, is set at 45%[30]. For simplicity, the flow velocity is assumed constant in the lateral direction of the channel, instead of a more realistic parabolic flow profile. Also transport of ions by diffusion is not considered. The average salt concentration measured with the impedance electrodes is calculated via the addition of the resistance of each element in a parallel configuration (see ESI figure S2). The resulting calculated signal from the impedance electrodes $C_{avg}(t)$ is plotted together with the local concentration $C(t)$ at the exit in figure 3. From these results we conclude that the desalination percentage measured with the impedance electrodes is 45%, while the maximum locally achieved desalination percentage reaches 97% at the outlet of the channel. The amount of desalination is therefore underestimated by more than a factor of 2.

3 Materials and Methods

3.1 Fabrication of the macro cell for control experiments

Control experiments are performed in a macro cell, which is shown in figure 4. This cell consists of two PMMA sheets with a u-shaped PDMS spacer (thickness 2.25 mm) clamped together. On each side of the spacer a sheet of carbon electrode material is placed. A reservoir with a volume of 0.45 ml is formed through the spacer and is illustrated by the dashed blue line in figure 4.

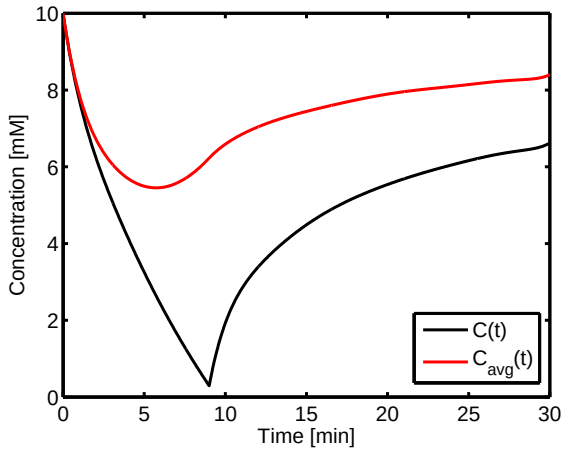

Fig. 3 Results from the element model calculations. $C(t)$ represents the concentration directly at the exit of the CDI cell for CDI on chip. The flow rate is 1 μL min^{-1}. $C_{avg}(t)$ represents the concentration as it is determined with the desalination electrodes. $C_{avg}(t)$ gives a maximum desalination percentage of 45% while the locally achieved desalination percentage is calculated at 97%.

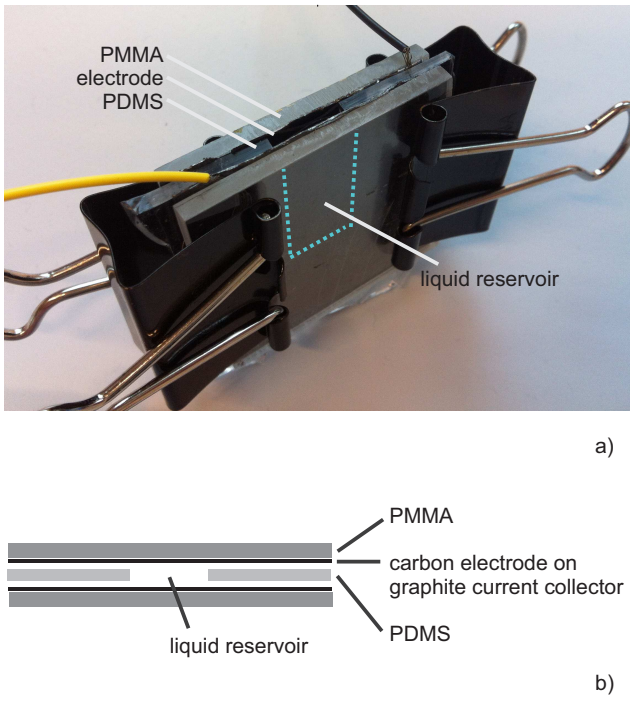

Fig. 4 Photo of the macrofluidic cell (a) and schematic cross-section of the cell as seen from the top (b). The cell consists of two polymethyl methacrylate (PMMA) sheets separated by a u-shaped spacer. The liquid volume of the liquid reservoir formed by the spacer is 0.45 ml. On each side of the spacer carbon electrode material is placed.

3.2 Fabrication of the microfluidic CDI chip through 3D rapid prototyping

The microfluidic CDI chip is fabricated from poldimethylsiloxane (PDMS)(type 182, Sylgard silicone elastomer, Dowcorning). The mold for PDMS casting is printed with a 3D printer in the material "clear resin"(Projet 6000HD, 3D Systems, USA). A schematic overview of the assembly of the chip is depicted in figure 1a. The microfluidic chip consists of two PDMS casts, top and bottom of the chip, which are bonded together using liquid PDMS. Bonding through liquid PDMS offers two advantages over more conventional plasma bonding. First, the longer curing time gives the experimenter more time to assemble the chip. Second, liquid PDMS corrects for small misalignments and therefore reduces the chance of leakages to occur. Figure 1b features the assembled chip. The distance between the electrodes is 1.5 mm. The height and length of the channel are 0.4 and 12 mm respectively, these are the same dimensions as the part of the electrodes that is exposed to the solution. A thin uniform layer of liquid PDMS is applied with a roller on the bottom half which contains the microfluidic channel. Both the top and bottom half contain slits for the electrode material. These electrodes are proprietary material from Voltea and consist of a sheet of graphite, forming the current collectors, coated with porous carbon[31]. The carbon is applied through casting a slurry of activated carbon mixed with a binder onto the graphite. They were stored in NaCl (obtained from Sigma Aldrich) solutions of equal molarity at least 24 hours prior to assembly of the chip. Before bonding of the chip, the electrodes are inserted in the slits. The electrode material is currently applied in industrial CDI devices from Voltea[31]. Their capacitance is therefore representative for current state-of-the-art CDI electrodes. Stainless steel wires are inserted through holes in the top half, up to reaching the electrodes and connect the chip to the potentiat (Bio-Logic SP−300, Claix, France). Liquid is inserted through a syringe pump (PHD 2000, Harvard Apparatus, MA, USA) via tubing (S−54−HL, Tygon® microbore tubing, Akron, Ohio). A picture of the chip is shown in figure 1c. A microscope (DMi 5000M, Leica, Wetzlar, Germany) with a color camera (ColorView 11, Soft Imaging Systems GmbH, Olympus, Tokyo, Japan) and BGR filter cube is used for fluorescence measurements.

3.3 Impedance spectroscopy with desalination electrodes

The salt concentration in the microfluidic channel is measured by impedance spectroscopy with the same electrodes that are used for desalination. Therefore, the applied potential on the electrodes consists of two components. The first component is the DC potential of 0.5 V for desalination. Note that this potential is lower than the typical 1.2 V at which a CDI cell often operates to ensure operation well within the non-faradaic window, thus minimizing the risk of a potential leakage current and possible pH change which might affect our fluorescence intensity in later experiments (section 4.3). The second component is an AC signal with an amplitude of 10 mV sweeped from 100 Hz to 3 MHz to obtain an impedance spectrum. Prior to the impedance measurements, the system is calibrated for NaCl solutions varying in molarity from 5 to 20 mM. Solutions were prepared with MilliQ water and experiments are performed at room temperature. Electrodes were settled in the measurement solution at least 24 hours prior to the experiments. This method is first verified with the macrofluidic desalination cell (fig. 4), filled with 10 mM NaCl. During the desalination cycle, samples with a volume of 2 μL are taken out of the cell and are externally analyzed by impedance spectrometry with a set of calibrated microfabricated interdigitated platinum impedance electrodes. A correction in the data is made for the increase in impedance caused by the sample extraction, due to a decrease of the water level in the fluidic cell. This results in a smaller contact area with the desalination electrodes, changing the cell constant and resulting in a slight increase in impedance.

3.4 Desalination on-chip

The performance of the CDI chip is first tested using a 10 mM NaCl solution for flow rates varying from 1 to 10 μL min^{-1}. To avoid time-consuming calibration, the calculated cell constant of the electrode configuration is used to obtain the concentration from the impedance measurements instead. The impedance of the chip is expected to be 2650 Ω if the channel is filled with a 10 mM NaCl solution. Due to variations in the geometry and electrode material from chip-to-chip, the cell constant may vary and variations of up to 39% have been observed. It is also noticed that the measured impedance shows an offset for different flow rates. Each measurement was corrected for this offset.

To demonstrate that CDI is applicable as a sample preparation method for biological samples, desalination of Fluorescein isothiocyanatedextran (FITC-dextran), average mol wt 4,000, (FITC:Glucose = 1:250) obtained from Sigma-Aldrich, in phosphate buffer is performed. The phosphate buffer consists of 3.3 mM KH_2PO_4 and 3.3 mM $K_2HPO_4 \cdot 3H_2O$ with a pH of 7.08. The concentration of FITC-dextran is 0.6 mM. The flow rate is controlled with the connected syringe pump and set at 1 μL min^{-1}. The CDI chip is charged through application of a potential of 0.5 V. To check that the concentration of FITC-dextran remains constant over time, fluorescent imaging is performed with time-intervals of several minutes. At the outlet the concentration is monitored via extraction of 5 μL samples which are taken every 5 min and analyzed with impedance spectrometry.

4 Results and discussion

4.1 Verification of online monitoring of the salt concentration in the macro cell

The reliability of online impedance measurements with desalination electrodes to determine the salt concentration in the solution during desalination was first confirmed in a macrofluidic cell (fig. 4) containing 10 mM NaCl. The results are shown in figure 5. The green line represents the applied potential for desalination. Starting at t = 18 min, a potential of 0.5 V is applied for 40 min. The blue line shows the results from the online impedance measurements performed with the desalination electrodes at a frequency of 11.7 kHz. The red circles represent the concentration as it is measured with the earlier described small samples reference method (see section 3.3). It can be observed that the measured starting concentration is 11.2 mM. This deviation from the inserted 10 mM might be due to experimental variations in solutions and release of ions from the carbon electrodes between the actual measurements and the calibration experiments. The minimum concentration reached in the cell is 8 mM at t = 58 min. The removed charge at this concentration variation results in a capacitance of 69 mF cm^{-2} according to the relation $Q = CE$. Where Q is the charge removed [C], C is the capacitance [F] and E is the applied potential [V]. After discharging at t = 58 min., the salt concentration does not make a full recovery to its initial value, but keeps decreasing slightly between t = 65 min and the end of the experiment. This discrepancy is likely due to transport of ions inside the carbon electrode material or wetting of the porous carbon. From previous experiments we observed that storing the electrodes in the ion solution of interest before measuring, minimizes this effect. However, a slight deviation from the externally analyzed samples is still visible. Overall the impedance and sampling methods show excellent experimental agreement.

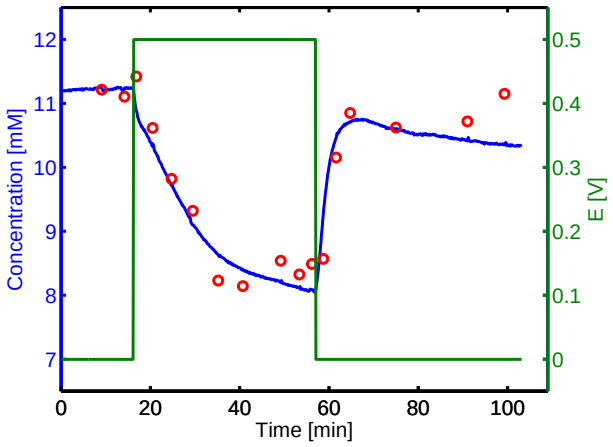

Fig. 5 Measured salt concentration as a function of time during a desalination cycle of the macro cell. The green line shows the applied desalination potential. The blue line represents the concentration obtained from impedance spectroscopy measurements with the desalination electrodes. These results agree well with the reference measurements, obtained from extracted samples (red circles).

4.2 Desalination and online monitoring of CDI on chip

After experimental verification of the impedance spectroscopy method to determine the salt concentration in the macrocell, this method is now applied to a chip to monitor the salt concentration between the electrodes online. A 10 mM NaCl solution is pumped in the chip. The impedance is calculated from the cell constant of the electrode configuration.

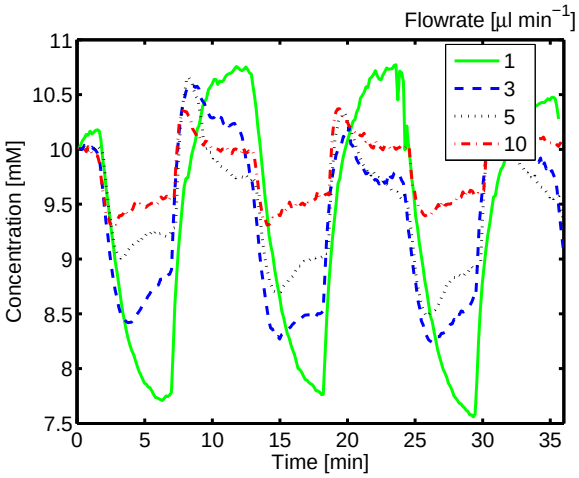

Fig. 6 Measured impedance over time at a frequency of 11.7 kHz. The applied desalination potential is 0.5 V, each cycle of charging and discharging takes 10 min. The flow rate varies from 1 to 10 μL min^{-1}.

In figure 6 the concentration as a function of time is plotted for different flow rates. As discussed in section 2.2, the measured concentration is an average of the concentration in the channel between the electrodes, from entrance to exit, and the actual extent of local desalination at the exit of the channel is twice the amount as observed here. The graph includes three charging and discharging cycles for desalination at a potential of 0.5 V. Each complete cycle (charging and discharging) lasts 10 min. The first cycle starts with charging of the cell at t = 2 min. A constant charging and discharging behavior is observed from the second cycle onwards. Applying a small AC signal with an amplitude of 10 mV on top of a DC desalination potential might help in increasing the charging and regeneration rate, as shown by Sharma et al.[32]. It is expected that the amount of desalination decreases as the flow rate in-

creases, simply because at higher flow rates more ions pass the desalination compartment, while the storage capacity of the electrodes remains constant. This hypothesis is confirmed by the results shown in figure 6. The desalination percentage of the system for all flow rates or different concentration ranges can be further improved through the following adjustments of the geometry. First, by increasing the surface-to-volume ratio, the relative storage capacitance of the electrodes is improved. This can be realized by narrowing the microfluidic channel, which at present is rather large (1.5 mm). A second method is to increase the residence time of the liquid in between the electrodes, e.g. by increasing the length of the electrodes and the channel.

4.3 CDI as sample preparation method: Desalination of a sample with FITC-dextran as a model compound

CDI can be used as an elegant sample preparation method for biological molecules. This is demonstrated through desalination on-chip of a FITC-dextran solution in phosphate buffer, see figure 7.

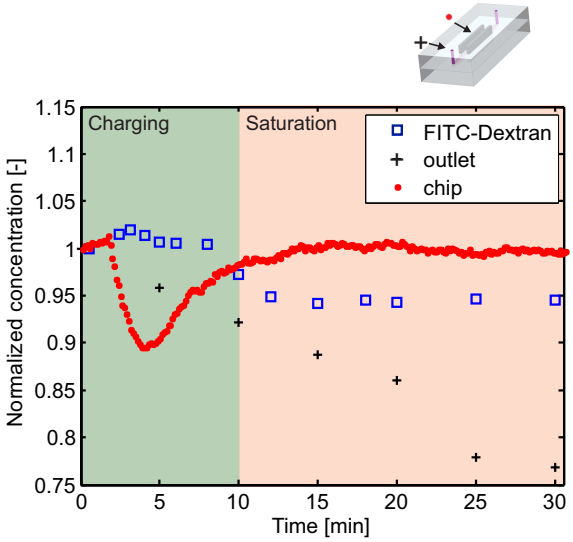

Fig. 7 This figure shows the desalination of FITC-dextran upon the application of a potential of 0.5 V starting at t = 2 min. and continuing for 30 minutes. The fluoresence intensity of FITC-dextran is plot in blue squares. The buffer concentration measured at the outlet is plot in black(+). The red dots represent the buffer concentration measured with the desalination electrodes. All values are normalized and experiments are performed with a flow rate of 1 μL min^{-1}. The observed drop in buffer concentration at the outlet of the chip is 23% after 30 min. The drop in fluorescence intensity of FITC-dextran is only 6% and most likely due to pH variations.

We have selected a simple non-adsorbing biological molecule to perform these proof-of-principle measurements. Future development of the chip requires testing with actual proteins, which vary in size, mobility and absorbing properties. This figure shows the normalized results of three simultaneous measurements. The concentration of FITC-dextran, measured with fluorescence microscopy is shown in blue squares. An example of a fluorescent image of the outlet of the chip can be found in the supplementary information, see figure S3. The variation in concentration of buffer is measured with the online impedance measurements as demonstrated in section 4.2 and plotted in red dots. Additionally the concentration variation of the solution is measured at the outlet of the chip, where samples of 5 μL are collected and analyzed with a set of impedance electrodes. These results are shown in black(+). Note that the outlet is located at a distance from the CDI electrodes, which is why a delay in the concentration dip is measured. The intensity of the FITC-dextran remains stable after a drop of 6% around t = 8-12 minutes. This is approximately 7 min after the dip in concentration variation measured with impedance spectroscopy, which is the expected amount of time for the reservoir to renew its volume of 7 μL. Capacitive removal of FITC-dextran from the solution would eventually result in the FITC-dextran concentration to return to its original value. Bleaching would lead to a gradual decrease of the observed intensity across the entire time-interval. Therefore it is expected that the intensity drop (blue squares) is caused by a variation in the pH. At the outlet of the chip a drop in buffer concentration of 23% is observed in 30 minutes, which is a higher desalination percentage than measured with the impedance electrodes on-chip of 11%. This is in agreement with the hypothesis that between the electrodes an average concentration is measured which is, during desalination, twice as high than locally at the exit of the channel. In figure 7, two clear regimes can be distinguished, a regime where EDL charging occurs (green background), with resulting desalination and a regime where the electrodes are saturated (red background). In practical applications the device would only be operated in the first approximate 5 to 7 minutes of the charging regime. The FITC-dextran concentration remains constant within this charging regime.

4.4 Model and experimental agreement

The desalination percentage between the electrodes of 11% is lower than we earlier observed for desalination of 10 mM NaCl at a flow rate of 1 μL min^{-1}, see figure 6. This is attributed to blockage of electrode pores by FITC-dextran which results in a decrease of the effective surface area and amount of ions absorbed. The CDI model, described in section 2.2, predicts an underestimation of the local desalination percentage at the exit of the electrodes of a factor of 2. Therefore the locally achieved desalination percentage is expected to reach 22%.

Thus we can conclude that the concentration of FITC-dextran remains constant over time, while the buffer concentration at the outlet is decreased by 23%. The percentage of desalination can be further improved through optimization of the geometry of the chip, as well as the pH and the ionic strength.

5 Conclusions

We have demonstrated that CDI can be used as an on-chip sample preparation method through desalination of a sample where FITC-dextran is used as a model compound. From our experiments we can conclude that the concentration of FITC-dextran remains constant over a time-span of 30 min, while the buffer concentration measured at the outlet of the chip is reduced by 23%. At the same time we have shown a novel method to measure the average online salt concentration on-chip, using impedance spectroscopy with the desalination electrodes. This method was first verified in a macrofluidic cell. The application of this method was demonstrated on-chip, through a variation in flow rate of the solution as well as a variation in the applied desalination potential. From these measurements we can confirm the hypothesis that the relative amount of salt removed from the liquid decreases as the flow rate increases. We also found a relation between the applied potential and the amount of charge stored at the electrodes. Future research should be directed towards improvement of the desalination efficiency. The setup can be optimized to increase the amount of salt removed from the sample through downsizing the channel width. Also pH and ionic strength can be varied to optimize the separation efficiency between salts and proteins. Moreover, samples can be flushed multiple times through the device (or multiple stages of identical devices) to reach down to even lower salt concentrations for example required for ESI-MS.

Acknowledgment

The authors thank the NWO (Netherlands Organization of Scientific Research (Spinoza Grant A. van den Berg) for financially supporting this research and dr.ir. M.A. van Damme for supporting the collaboration. The authors like to thank Menno van Rooijen for fruitful discussions and his preliminary work on the characterization of the macro cell for CDI. We would like to extend our gratitude to Voltea for supplying the activated carbon electrode material. We declare no conflict of interest.

References

1 T.-C. Chao and N. Hansmeier, *Proteomics*, 2013, **13**, 467–479.
2 J. M. Labuz and S. Takayama, *Lab Chip*, 2014, **14**, 3165–3171.
3 J. Martnez-Aguilar, J. Chik, J. Nicholson, C. Semaan, M. J. Mckay and M. P. Molloy, *Proteomics - Clinical Applications*, 2013, **7**, 42–54.
4 F. Xiang, Y. Lin, J. Wen, D. W. Matson and R. D. Smith, *Analytical Chemistry*, 1999, **71**, 1485–1490.
5 D. Gao, H. Liu, Y. Jiang and J.-M. Lin, *Lab Chip*, 2013, **13**, 3309–3322.
6 A. E. Ashcroft, *Nat. Prod. Rep.*, 2003, **20**, 202–215.
7 N. Lion, V. Gobry, H. Jensen, J. S. Rossier and H. Girault, *Electrophoresis*, 2002, **23**, 3583–3588.
8 Y. Chen, M. Mori, A. C. Pastusek, K. A. Schug and P. K. Dasgupta, *Analytical Chemistry*, 2011, **83**, 1015–1021.
9 N. Jehmlich, C. Golatowski, A. Murr, G. Salazar, V. M. Dhople, E. Hammer and U. Voelker, *Clinica Chimica Acta*, 2014, **434**, 16–20.
10 A. W. Bell, E. W. Deutsch, C. E. Au, R. E. Kearney, R. Beavis, S. Sechi *et al.*, *Nature Methods*, 2009, **6**, 423–430.
11 A. Dodge, E. Brunet, S. Chen, J. Goulpeau, V. Labas, J. Vinh and P. Tabeling, *Analyst*, 2006, **131**, 1122–1128.
12 R. L. Gundry, M. Y. White, C. I. Murray, L. A. Kane, Q. Fu, B. A. Stanley and J. E. Van Eyk, in *Preparation of Proteins and Peptides for Mass Spectrometry Analysis in a Bottom-Up Proteomics Workflow*, John Wiley & Sons, Ltd., 2001.
13 Y. Jiang, P.-C. Wang, L. E. Locascio and C. S. Lee, *Analytical Chemistry*, 2001, **73**, 2048–2053.
14 N. Xu, Y. Lin, S. A. Hofstadler, D. Matson, C. J. Call and R. D. Smith, *Analytical Chemistry*, 1998, **70**, 3553–3556.
15 P.-C. Wang, D. DeVoe and C. Lee, *Electrophoresis*, 2001, **22**, 3857–3867.
16 J. W. Blair and G. W. Murphy, in *Electrochemical Demineralization of Water with Porous Electrodes of Large Surface Area*, ch. 20, pp. 206–223.
17 A. M. Johnson and J. Newman, *Journal of The Electrochemical Society*, 1971, **118**, 510–517.
18 T. J. Welgemoed and C. F. Schutte, *Desalination*, 2005, **183**, 327–340.
19 K. S. Chae and A. M. Lenhoff, *Biophysical Journal*, 1995, **68**, 1120–1127.
20 S. Koster and E. Verpoorte, *Lab Chip*, 2007, **7**, 1394–1412.
21 F. T. van den Brink, L. Büter, M. Odijk, W. Olthuis, U. Karst and A. van den Berg, *Analytical Chemistry*, accepted for publication, 10.1021/ac503384e.
22 S. Porada, R. Zhao, A. van der Wal, V. Presser and P. Biesheuvel, *Progress in Materials Science*, 2013, **58**, 1388 – 1442.
23 O. N. Demirer and C. H. Hidrovo, *Microfluidics and Nanofluidics*, 2014, **16**, 109–122.
24 M. E. Suss, P. M. Biesheuvel, T. F. Baumann, M. Stadermann and J. G. Santiago, *Environmental Science & Technology*, 2014, **48**, 2008–2015.
25 R. Zhao, M. van Soestbergen, H. Rijnaarts, A. van der Wal, M. Bazant and P. Biesheuvel, *Journal of Colloid and Interface Science*, 2012, **384**, 38–44.
26 S. H. Roelofs, M. van Soestbergen, M. Odijk, J. C. T. Eijkel and A. van den Berg, *Ionics*, 2014, 1–8.
27 C. Huang, T. Xu, Y. Zhang, Y. Xue and G. Chen, *Journal of Membrane Science*, 2007, **288**, 1 – 12.
28 T. Xu and C. Huang, *AIChE Journal*, 2008, **54**, 3147–3159.
29 M. A. Anderson, A. L. Cudero and J. Palma, *Electrochimica Acta*, 2010, **55**, 3845 – 3856.
30 R. Zhao, P. M. Biesheuvel, H. Miedema, H. Bruning and A. van der Wal, *The Journal of Physical Chemistry Letters*, 2010, **1**, 205–210.
31 http://www.voltea.com.
32 K. Sharma, R. T. Mayes, J. O. Kiggans Jr., S. Yiacoumi, H. Z. Bilheux, L. M. H. Walker, D. W. Depaoli, S. Dai and C. Tsouris, *Separation and Purification Technology*, 2014, **129**, 18–24.